Accepted Manuscript

Title: Application of miscibility analysis and determination of Soluplus solubility map for development of carvedilol-loaded nanofibers

Authors: Olivera Kaljević, Jelena Djuris, Bojan Čalija, Zoran Lavrič, Julijana Kristl, Svetlana Ibrić

PII: S0378-5173(17)30427-1
DOI: http://dx.doi.org/doi:10.1016/j.ijpharm.2017.05.017
Reference: IJP 16665

To appear in: *International Journal of Pharmaceutics*

Received date: 14-1-2017
Revised date: 19-3-2017
Accepted date: 6-5-2017

Please cite this article as: Kaljević, Olivera, Djuris, Jelena, Čalija, Bojan, Lavrič, Zoran, Kristl, Julijana, Ibrić, Svetlana, Application of miscibility analysis and determination of Soluplus solubility map for development of carvedilol-loaded nanofibers.International Journal of Pharmaceutics http://dx.doi.org/10.1016/j.ijpharm.2017.05.017

Application of miscibility analysis and determination of Soluplus solubility map for development of carvedilol-loaded nanofibers

Olivera Kaljević[a]*, Jelena Djuris[a], Bojan Čalija[a], Zoran Lavrič[b], Julijana Kristl[b], Svetlana Ibrić[a]

[a] Faculty of Pharmacy, University of Belgrade, Vojvode Stepe 450, 11221 Belgrade, Serbia

[b] Faculty of Pharmacy, University of Ljubljana, Aškerčeva 7, 1000 Ljubljana, Slovenia

***Corresponding author: Olivera Kaljević**

Department of Pharmaceutical Technology and Cosmetology

Faculty of Pharmacy

University of Belgrade

Vojvode Stepe 450

11221 Belgrade, Serbia,

Tel: +38-164-4090618

Email: oliverak@pharmacy.bg.ac.rs

Graphical Abstract

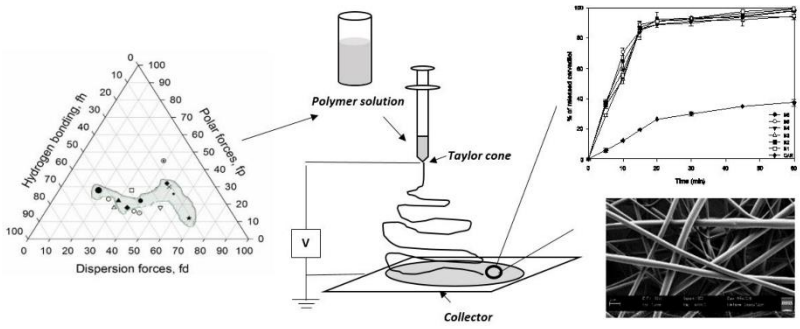

Abstract

Electrospinning was used to produce carvedilol-loaded Soluplus polymer nanofibers using a systematic approach. Miscibility between drug and polymer was determined through calculation of the interaction parameter, χ, and the difference between the total solubility parameters, $\Delta\delta_t$. A solubility map for Soluplus was obtained by examining different solvent systems, carrying out electrospinning, and characterizing the nanofibers formed. Miscibility studies showed that carvedilol and Soluplus can form a miscible system (χ = -2.3054; $\Delta\delta_t$ <7.0 $MPa^{1/2}$). Based on the Soluplus solubility map, acetone: chloroform (90:10; w/w) represents a suitable solvent system for electrospinning of carvedilol-loaded Soluplus nanofibers. Scanning electron microscopy of these nanofiber samples showed smooth surface morphology. The nanofibers had a regular cylindrical morphology. Beads appeared along the nanofibers more frequently in formulations with lower percentages of carvedilol. Differential scanning calorimetry showed no melting endothermic peak for carvedilol, which suggests its complete conversion from the crystalline to the amorphous form (at polymer: carvedilol 1:1). The infrared spectrum of the carvedilol-loaded Soluplus nanofibers showed no characteristic carvedilol peak at 3344.5 cm^{-1}, which suggests interactions between carvedilol and Soluplus. Dissolution studies of these nanofibers showed improved pure carvedilol dissolution properties, with >85% of the carvedilol released in the first 15 min, *versus* 20% for pure carvedilol. The use of miscibility analysis and polymer solubility studies demonstrate great technological potential to tackle the challenge for inadequate dissolution of poorly water-soluble drugs.

Keywords: poorly soluble drugs; ; ; ; ; , solvent mapping, electrospinning, solid dispersions, solubility enhancement, interaction parameter

1. Introduction

Electrospinning has become one of the most used modern methods for nanofiber production for different fields of application (Reneker and Yarin, 2008). Electrospinning is also one of the most frequently used techniques for preparation of solid dispersions of poorly soluble drugs and polymers. During electrospinning, a polymer solution or 'melt' is subjected to very high electrostatic forces. This induces a charge on the surface of the liquid. Mutual charge repulsion causes a force directly opposite to the surface tension. As the intensity of the electric field is increased, the hemispherical surface of the fluid at the tip of the capillary tube elongates to form a conical shape known as the Taylor cone (the base region). With increasing field, a critical value is attained when the repulsive electrostatic force overcomes the surface tension and a charged jet of fluid is ejected from the tip of the Taylor cone. The ejection of the polymer solution from a nozzle is followed by random deposition of the polymer nanofibers on an electrically grounded collector (Luo et al., 2010; Pham et al., 2006).

A large number of factors can influence the critical quality attributes of the final product here, the nanofibers, such as nanofiber diameter and morphology, and number of beads on the nanofiber surface. These factors include the formulation parameters (e.g., type and concentration of polymer, solvent and solution properties), the process parameters (e.g., applied voltage, flow rate, collector distance, size of nozzle orifice), and the ambient conditions (e.g., relative humidity, temperature) (Pelipenko et al., 2015; Luo et al., 2010; Wannatong et al., 2004). A careful balance between these factors thus needs to be achieved to obtain stable electrospinning rather than electrospraying. The main difference in electrospraying is that the ejected jet breaks down into droplets, usually as a consequence of using a lower concentration of polymer solution than what is used in electrospinning. Consequently, electrospinning produces nanofibers while particles are dominant with electrospraying (Chakraborty et al., 2009). During electrospinning, a stable Taylor cone needs to be obtained, which again depends

on a number of parameters (Reneker and Chun, 1996; Pham et al., 2006). Apart of solution properties, several process parameters may have the influence on the electrospinning, and they need to be monitored. For example, if higher voltage is applied, it can result in smaller and less stabile Taylor cone, but also will lead to greater stretching of the solution and to reduction of the fiber diameter. Also, for a given voltage, there is a corresponding flow rate, if a stabile Taylor cone is to be maintained, where the increase of the flow rate can lead to increase in the fiber diameter. This indicates that all parameters are connected and have complex influence on the electrospinning (Ramakrishna, 2005). Thus polymer solutions that are considered suitable for electrospinning need to provide continuous nanofiber production, a stable Taylor cone, uniform nanofiber morphology, and minimal 'beads-on-a-string' structure (Luo et al., 2010; Mahalingam et al., 2015; Pham et al., 2006).

Nanofibers obtained by electrospinning basically represent solid dispersions that can improve the dissolution properties of poorly soluble drugs (Vo et al., 2013; Nagy et al., 2012, 2015; Paaver et al., 2014). The phase behavior of a drug and polymer system can be very complicated, as the drug can be present in a crystalline form (i.e., as one or more polymorphic forms), or partially or completely amorphous forms (Vasconcelos et al., 2007). The degree of miscibility between drug and polymer in a blended system is extremely important for stabilization of the amorphous drug–polymer system, as it is generally believed that miscibility at the molecular level is necessary to achieve maximum physical stabilization, as well as enhanced solubility (Marsac et al., 2006; Djuris et al., 2013; Meng et al., 2015). One of the methods for miscibility evaluation is based on determination of the Flory–Huggins interaction parameter, χ. This can be achieved through a description of the mixing thermodynamics in drug and excipient systems using Flory–Huggins lattice theory and the melting point depression method. Another approach for miscibility evaluation is based on the group contribution

method, as modified by Hansen, and this is based on determination of the difference in the total solubility parameter, $\Delta\delta_t$, between the two components (Meng et al., 2015).

At the same time, the solubility parameters can be useful for selection of the appropriate solvent for a polymer, to ensure successful electrospinning (Luo et al., 2012). A suitable solvent system for an active pharmaceutical ingredient and a selected polymer needs to be based on a solvent that can dissolve them both, and that has further properties that are relevant for the electrospinning (e.g., its relative permittivity, dielectric constant, evaporation rate). Solvents with different solubility properties can influence the polymer chain conformation and viscoelasticity, the critical minimum concentration of the polymer in solution, the nanofiber diameter, the loaded drug crystallinity, and the electrospun polymeric nanofiber tensile strength and morphology (Mahalingam et al., 2015).

Literature sources and technical reports offer different ways to estimate and illustrate solubility parameters, which includes the triangular graph (Barton, 1983; Burke, 1984), which is frequently the main tool used to select solvents for electrospinning (Hansen, 2007; Luo et al., 2010, 2012). Based on the suitable range of values of dielectric constant of solvents within the surface drawn in the triangular graph, solvents can be defined in terms of how well they dissolve the active pharmaceutical ingredient and the polymer. By overlapping the desired properties of potential solvents, the most suitable for electrospinning with the selected active pharmaceutical ingredient and polymer can be determined. However, the literature has noted frequently that although a solvent can dissolve a polymer of interest well, this does not guarantee that the resulting solution can be used to make nanofibers by electrospinning (Luo et al., 2010).

Thus considering all of the characteristics mentioned above, it is necessary to apply a more organized approach to reach the definition of the final product in the easiest and most consistent way. Apart from the solubility issues, there are also a great number of material

attributes and process parameters that need to be taken into consideration; however, more importantly, these should not be looked at separately, but be part of a systematic procedure.

The aim of the present study was to apply miscibility preformulation studies to prepare and characterize nanofibers by electrospinning with carvedilol and Soluplus polymer. Although carvedilol and Soluplus have been investigated in studies on electrospinning (Nagy et al., 2012; Paaver et al, 2014; Balogh et al., 2015), to the best of our knowledge there have been no previous reports of combined miscibility studies as applied to the production of solid dispersions in the form of nanofibers. The miscibility of carvedilol and Soluplus polymer was thus analyzed through determination of their solubility and interaction parameters, with these solubility parameters further used for construction of the polymer solubility map. A suitable solvent system for Soluplus polymer was determined using a triangular graph based on the solubility parameters, which was supported also by the relevant carvedilol solubility and relative permittivity for electrospinning. The successful electrospinning of these carvedilol-loaded Soluplus nanofibers was followed by their characterization.

2. Materials and methods

2.1. Materials

Carvedilol (European Pharmacopoeia, vol. 8) was used as a model drug and it was obtained from commercial supplier (Hemofarm, Belgrade, Serbia). Polyethylene glycol–polyvinyl caprolactam–polyvinyl acetate grafted copolymer (Soluplus) was kindly donated by the manufacturer (BASF, Germany). Acetic acid, acetone, acetonitrile, 1-buthanol, chloroform, ethanol, ethylene glycol, formic acid, glycerol, methanol, 1-propanol, 2-propanol, methyl isobutyl ketone, ethyl acetate, and hydrochloric acid were from Sigma-Aldrich (Poole, UK).

2.2. Investigation of carvedilol–Soluplus miscibility

2.2.1. Determination of the interaction parameter

Physical mixtures of carvedilol and Soluplus were prepared to determine the interaction parameter, χ, based on Flory–Huggins lattice theory. These were prepared as 10 g of each mixture by manual addition of carvedilol and Soluplus to different carvedilol percentages, as (in g, with percentage carvedilol indicated): 0.5:9.5 (5%); 1:9 (10%); 2:8 (20%); 3:7 (30%); 4:6 (40%); 5:5 (50%); 6.5:3.5 (65%); and 8:2 (80%).

These physical mixtures underwent thermal analysis by differential scanning calorimetry (DSC; see section 2.4.3.2.) The onset of melting for the physical mixtures was taken as the extrapolated onset of the bulk melting endotherm. The Flory–Huggins interaction parameter, χ, was calculated through linear regression analysis of Equation (1):

$$\frac{1}{Tmix} - \frac{1}{Tpure} = -\frac{R}{\Delta Hfus}\left[ln\phi_{API} + \left(1 - \frac{1}{m}\right)\phi_{polymer} + \chi\phi_{polymer}\right] \quad (1),$$

where *Tmix* and *Tpure* are the melting points of the physical mixture and the pure drug, respectively, ΔH_{fus} is the heat of fusion of the pure drug, ϕ_{API} and $\phi_{polymer}$ are the volume fractions of the drug (i.e., active pharmaceutical ingredient) and polymer, respectively, and *m* is the ratio of the volume of the polymer to that of the drug. χ is an interaction parameter that accounts for the enthalpy of the mixing, and it provides an indication of the drug–polymer miscibility. *Tmix* and *Tpure* were obtained from the thermograms. These data are given as a function of the square of the volume fraction of the polymer from the rest of Equation (1), where the interaction parameter was calculated as the slope of the fitted curve presented by this function.

2.2.2. Determination of solubility parameters

For determination of the solubility parameters, those of Hansen were used (Hansen, 2007). The total solubility parameter δ_t was determined from the contribution of interactions between the dispersion forces, δ_d, the polar interactions, δ_p, and the hydrogen bonding, δ_h, of the functional groups. The solubility parameters for carvedilol were calculated using the group-contribution method of Stefanis and Panayiotou (2012). The molecular structure of each organic compound

can be described using two kinds of functional groups: first-order groups (e.g., CH_3–, –CH_2–, C≡C), which describe the basic molecular structure of a compound; and second-order groups (e.g., $(CH_3)_2$–CH–, $(CH_3)_3$–C–, $CH_3(CO)CH_2$–), which significantly improve the accuracy of predictions (Stefanis and Panayiotou, 2012). The Hansen solubility parameters for carvedilol were calculated according to Equations (2) to (4), which apply for values >3 $MPa^{1/2}$:

$$\delta_d = (\sum_i NiCi + \sum_j MjDj + 959.11)^{0.4126} \text{ MPa}^{1/2} \quad (2),$$

$$\delta_p = (\sum_i NiCi + \sum_j MjDj + 7.6134) \text{ MPa}^{1/2} \quad (3),$$

$$\delta_h = (\sum_i NiCi + \sum_j MjDj + 7.7003) \text{ MPa}^{1/2} \quad (4),$$

where C_i is the contribution of the first-order group of type i that appears N_i times in the compound, and D_j is the contribution of the second-order group of type j that appears M_j times. The values for each group for the calculation of the carvedilol solubility parameters were obtained from the literature (Stefanis and Panayiotou, 2012). The solubility parameters for Soluplus were also obtained from the literature (Djuris et al., 2013). The difference between the total solubility parameters, $\Delta\delta_t$, of the drug and the polymer was determined by calculation of the total solubility parameter for the drug and polymer according to Equation (5):

$$\delta_t^2 = \delta_d^2 + \delta_p^2 + \delta_h^2 \quad (5).$$

The drug–polymer miscibilities were classified on the basis of the difference, $\Delta\delta_t$, between the total solubility parameters of the drug and the polymer.

2.3. Mapping the solubility region of Soluplus on the triangular graph

Based on preliminary experiments where different amounts of Soluplus were dissolved in chosen solvents, and on a literature review, 20% (w/w) Soluplus was chosen as the optimal polymer concentration for this purpose. The solvent positions on the triangular graph are identified by their fractional parameter values, which can be obtained from the literature (Barton, 1983) or calculated as shown for the example in Table 1. These fractional parameters

were suggested by Teas (1968), as f_d, f_p, and f_h, and they can be derived mathematically from the dispersion forces component δ_d, the polar force component δ_p, and the hydrogen bonding component δ_h of the Hansen parameters, respectively. The triangular graph expresses the fractional parameters as a ternary plot that is drawn as a triangle. Each side of this graph represents a distinct variable and has a scale from 0 to 100 (Barton, 1983). The solubility of 20% (w/w) Soluplus was tested for 15 different solvents. The mixtures were stirred with a magnetic stirring bar. The degree of swelling or dissolution was visually assessed after stirring for 10 min, 1 h, and 24 h. The observed solubility was categorized and recorded as 'partial' or 'high'. The solubility map of Soluplus was constructed by drawing a contour area around points with high 24-h solubility test results of the selected solvents on the triangular graph. Further selection of the optimal solvent system for electrospinning of carvedilol and Soluplus polymer here was based on the dielectric constant and the possibility of the solvent system to dissolve carvedilol (from values reported in the literature or determined experimentally), as well as on the results obtained from the triangular graph (Smallwood, 1996). The solvent systems from the contoured area in the triangular graph in which carvedilol was soluble also underwent electrospinning (data not shown). Five solvent systems were chosen considering the overlap of these desired properties, in terms of the suitability for dissolving carvedilol, and the convenience of the dielectric constant for electrospinning using the solvents mapped on the triangular graph. Electrospinning was then performed for these five solvent systems.

[a], according to Teas (1968)

2.4. Preparation of carvedilol–Soluplus solid dispersions by electrospinning

2.4.1. Preparation of the Soluplus polymer solution

According to the mapping on the triangular graph, the dielectric constant, and the carvedilol solubility, the solvent mixture of acetone and chloroform in the weight ratio of 9:1 was used for preparation of the 20% (w/w) Soluplus solution. The solution was stirred for 2 h using a

magnetic stirrer, at room temperature. Carvedilol was then added to obtain 5%, 10%, 20%, 30%, 40% and 50% (w/w) solutions in the 20% (w/w) Soluplus, based on the dry weight of the Soluplus polymer, and the solutions were stirred for an additional hour prior to electrospinning.

2.4.2. Electrospinning

Electrospinning of the carvedilol–Soluplus solutions was performed using an electrospinner (Fluidnatek LE-100; Bioinici, Valensia, Spain) with the process parameters set-up according to the carvedilol percentages, as shown in Table 2. For all of the experiments, the nozzle diameter was 0.6 mm and the collector distance was set at 15 cm. The temperature and relative humidity were strictly controlled, at 25 °C and 45%, respectively. The solvent for all of these formulations was acetone: chloroform, 9:1 (w/w).

2.4.3. Nanofiber characterization

The nanofibers obtained in the solvent system screening phase were evaluated using optical microscopy (Carl Zeiss Jena, Germany). The nanofibers produced were also characterized in detail by scanning electron microscopy (section 2.4.3.1.), DSC (section 2.4.3.2.), Fourier transform infrared spectroscopy (FTIR; section 2.4.3.3.), and *in-vitro* dissolution (section 2.4.3.4.).

2.4.3.1. Scanning electron microscopy

Morphological examination of the electrospun nanofibers was performed using scanning electron microscopy (Supra35 VP; Carl Zeiss, Oberkochen, Germany) operated at an accelerating voltage of 1 kV and with a secondary-electron detector. The nanofibers were fixed onto metal studs with double-sided conductive tape, with no coating applied prior to imaging. The diameters of 100 randomly selected nanofibers were measured using the ImageJ 1.44p software (National Institutes of Health, USA), for the mean nanofiber diameter.

2.4.3.2. Differential scanning calorimetry

Differential scanning calorimetry was used for characterization of the solid state and identification of the crystal and/or amorphous states of carvedilol. DSC was performed using a DSC 1 STAR^e system (Mettler Toledo GmbH Analytical, Giessen, Germany) under a pure nitrogen flux of 50 mL/min, and with a heating rate from 25 °C to 200 °C of 10 °C/min. Each sample was accurately weighed (6-10 mg) in an aluminum pan, which was then crimped and sealed. Temperature calibration was carried out using indium.

2.4.3.3. Fourier transform infrared spectroscopy

Fourier transform infrared spectroscopy was used to qualitatively characterize the interactions between carvedilol and Soluplus. The FTIR spectra of carvedilol, Soluplus, and the carvedilol-loaded Soluplus nanofibers were produced using an attenuated total reflectance accessory (Nexus, Thermo Nicolet, Madison, USA), in the range of 600 cm^{-1} to 4000 cm^{-1}, and with a resolution of 2 cm^{-1}.

2.4.3.4. *In-vitro* dissolution

In-vitro dissolution studies were carried out in 0.1 N hydrochloric acid (900 mL) at 37 ±0.5 °C using a United States Pharmacopeia method II dissolution tester (USP II, Erweka DT 600; Hausenstamm, Germany). Soluplus nanofibers containing 12.5 mg carvedilol were gently placed in modified sinkers and put in the vessel. The paddle rotation was 50 rpm, and aliquots of dissolution medium were withdrawn over a total period of 1 h (at 5, 10, 15, 20, 30, 45, 60 min). The carvedilol content was determined using a UV/VIS spectrophotometer (Evolution 300; Thermo Fisher Scientific, Loughborough, USA), at a detection wavelength of 241 nm.

3. Results and discusion

3.1. Carvedilol and Soluplus miscibility

The first method used for estimation of carvedilol and Soluplus miscibility was based on determination of the Flory–Huggins interaction parameter and the melting point depression phenomena, through examination of the physical mixtures prepared. Thermal analysis was

carried out, and the DSC thermograms of pure carvedilol and Soluplus and the carvedilol–Soluplus physical mixtures are shown in Figure 1.

The temperature of the onset of the carvedilol melting point was determined from these thermograms (Fig. 1). Initially, these data showed that this decreased with increased Soluplus content, which was already indicative of miscibility between carvedilol and Soluplus (Fig. 2.). From 10% to 20% carvedilol (Fig. 2, F2/F3), the change in the temperature of the onset of the carvedilol melting point was greater, so additional formulations containing 12.5%, 15%, and 17.5% carvedilol were prepared and examined to define more precisely the behavior and changes in this parameter (Fig. 2, F1p, F2p, F3p). The decreasing trend in the temperature of the onset of the carvedilol melting point was confirmed from the changes seen for these additional formulations.

The linear relationship over this range of the polymer weight fractions allowed for estimation of the interaction parameter, χ (Fig. 3). A positive χ indicates immiscibility, while a negative χ usually indicates miscibility of a system. Quantitatively, a greater negative χ indicates higher miscibility (Marsac et al., 2006, 2009; Meng et al., 2015). The slope of the fitted line shown in Figure 3 defines χ, which was calculated as -2.305. This negative value of χ indicates miscibility of carvedilol and Soluplus.

The second approach to analyze carvedilol–Soluplus miscibility was to calculate the difference between the corresponding solubility parameters, as indicated by Equation (5). Here, for $\Delta\delta_t$ <7.0 $MPa^{1/2}$, miscibility is likely to occur, whereas for $\Delta\delta_t$ >7.0 $MPa^{1/2}$, it is not (Greenhalgh et al., 1999). The Hansen solubility parameters for Soluplus were taken from the literature (Djuris et al., 2013), and for carvedilol they were calculated using Equations (2) to (4), as given in Table 3. According to the differences between these solubility parameters for carvedilol and Soluplus, the predominant types of interactions in this system are dispersion forces and hydrogen bonding. The difference in the total solubility parameters, $\Delta\delta_t$, of

carvedilol and Soluplus was 2.9 $MPa^{1/2}$, which is below the border for miscibility between two materials, and thus it is very likely that miscibility will occur (Greenhalgh et al., 1999). This is supported on the basis that Soluplus is an excipient with amphiphilic properties that was developed as a matrix polymer for solid solutions, and it can increase the solubility of poorly soluble active pharmaceutical ingredients by forming miscible systems (Hardung et al., 2010).

At this point, according to these descriptive and numerical methods, these data showed that the carvedilol–Soluplus system indeed promotes miscibility; i.e., carvedilol and Soluplus are miscible. ***3.2. Mapping the solubility region of Soluplus on the triangular graph***

As the solvent positions on the triangular graph are unique and invariable, if a given polymer is tested for solubility across a selection of solvents while other variables are kept constant, such as the solution concentration, operating temperature, and pressure constant, the solubility region of the polymer can be defined on the triangular graph. This empirically determined solubility region, i.e., the range of the solvents on the triangular graph, provides a valuable means for selection of a solvent system that can dissolve the chosen polymer and will thus be suitable for electrospinning (Luo et al, 2010). Solvents that lie in the contoured area on the graph can be further analyzed from the aspect of their suitability for electrospinning with the chosen active pharmaceutical ingredient.

Based on 15 different solvent systems with diverse solubility parameters and different functional groups, the triangular graph for Soluplus was constructed (Fig. 4). During the testing of the Soluplus solubility in the chosen solvents/ solvent mixtures, partial or high solubility of Soluplus over the 24-h testing period was observed, mainly due to the polymer amphiphilic properties. In Figure 4, the filled-in symbols represent solvents where Soluplus is highly soluble, while the open symbols represent solvents where Soluplus was partially soluble. Thus the shaded area in Figure 4 includes the solvents that have the required solubility parameters for dissolving the Soluplus polymer.

These solvents given in the triangular graph of Figure 4 were then investigated in more detail. Their dielectric constants were defined (Smallwood, 1996), and the solvents with very high (>35) or very low (<15) dielectric constants (e.g., water, acetic acid, chloroform) were eliminated from the investigation, based on problems observed in the literature and on our experience. Literature data also showed that polycaprolactone nanofibers of <100 nm diameter were obtained when the dielectric constant of the solvent system used was approximately 19, and when this increased, the diameter of these nanofibers decreased (Luo et al., 2012).

Following this selection, the remaining potential solvents were compared in terms of their carvedilol solubility, with the solvents for carvedilol indicated as "S" in Table 4, and those showing little or no carvedilol solubility indicated as "I". (Table 4). The final selection for the suitability for electrospinning was thus defined by the solvents in which carvedilol can dissolve (Table 4, acetone, chloroform, acetone: chloroform 90:10 [w/w], acetone: chloroform 70:30 [w/w], ethanol, methanol).

These five chosen solvent systems were then used for electrospinning of carvedilol-loaded Soluplus nanofibers. Their suitability here was defined by the stability of the Taylor cone during the electrospinning, and by the appearance of the nanofibers obtained under optical microscopy (i.e., presence of beading) (Fig. 5). The solution with pure chloroform was eliminated because of its high evaporation rate, which resulted in the occasional drying of the nanofibers at the needle tip, and also because of the unstable process and the associated toxicity. Large differences between the solubility parameters of Soluplus and the solvent system were responsible for the beads-on-a-string morphology (Wannatong et al., 2004).

Charges present during electrospinning have greater effects on a polar solvent than a nonpolar solvent. The dielectric constant is related to the dipole moment, and it generally reflects the polarity of a molecule, which is also reflected in a higher value of the fractional

parameter, *fp*. This is a better predictor of electrospinning productivity than the dipole moment or other solvent properties (e.g., boiling point, density) (Wanatong et al., 2004).

Carbon tetrachloride does not show polarity, and it has not been reported as a successful solvent for electrospinning (Wannatong et al., 2004; Son et al., 2004). It is considered that a solvent with a higher dielectric constant has a higher net charge density in solution. As the charges carried by the jet increase during electrospinning, higher elongation forces are imposed by the jet under the electrical field, which results in smaller beads and thinner nanofiber diameter (Son et al., 2004).

The chosen electrospinning systems with solvent dielectric constants of approximately 19 produced nanofibers, while for the acetone–Soluplus solution (dielectric constant, 20.6), beads were observed. This was most likely because of the low boiling point of acetone, which caused the nozzle to become clogged up, producing an unstable process, and deformed nanofiber morphology (Augustine et al., 2016; Jaeger et al., 1998). In this phase, the 9:1 mixture (w/w) of acetone and chloroform was seen to be optimal in terms of the stability of the electrospinning and the appearance of the nanofibers in the preliminary testing. The combination of these two solvents changed the properties of the final solvent system, which overcame the solvent disadvantages and allowed stable electrospinning. This approach thus provided the possibility to develop a binary solvent system for the formation of nanofibers by electrospinning. The solubility–spinnability map simplified the solvent selection process by allowing mixed solvent systems to be developed for electrospinning.

[a], S, soluble; I not soluble

3.3. Preparation of carvedilol-loaded Soluplus nanofibers by electrospinning

During the electrospinning, this selected solvent system (i.e., acetone: chloroform, 9:1 [w/w]) provided a stable Taylor cone and a stable process overall. Here, this showed that a maximum

of 50% carvedilol (based on the dry weight of the Soluplus), could be incorporated into the carvedilol-loaded Soluplus nanofibers.

3.3.1. Morphology of the nanofibers

Scanning electron microscopy of the nanofibers is shown in Figure 6. The surface morphology of the nanofibers was smooth, but a trend for beads appearance was noted as more likely in formulations with the lower percentages of carvedilol. Pure Soluplus nanofibers were easy to produce with no bead formed (data not shown). The obtained fibers had a regular, cylindrical morphology. The average diameter of the nanofibers was <1 μm for all of the formulations tested from Table 2. The stable electrospinning and stable Taylor cone, and the morphologic characteristics of the nanofibers, indicated that this chosen solvent system in combination with the Soluplus polymer is suitable for these purposes.

3.3.2. Differential scanning calorimetry

Differential scanning calorimetry was performed for the nanofibers, and representative thermograms for up to 50% carvedilol are shown in Figure 7. This analysis was carried out to evaluate the transformation of the carvedilol during the formation of these carvedilol-loaded Soluplus nanofibers by electrospinning, as a solid dispersion. The isolated peak for carvedilol was not seen in any of these samples (Fig. 7), which implies that the carvedilol was in an amorphous form or was dissolved in the Soluplus, as was predicted by the evaluation of the carvedilol–Soluplus miscibility. As illustrated in Figure 7, the pure carvedilol was characterized by a single, sharp melting endothermic peak at 119.12 °C, which corresponded to the melting point of carvedilol, thus confirming its crystalline form. Based on the DSC measurements for all of the formulations given in Table 2, it can be concluded that the carvedilol-loaded Soluplus nanofibers produced contained carvedilol in a noncrystalline form, or to be more precise, in its amorphous form, for the range up to the 1:1 carvedilol:Soluplus

ratio (i.e., 50% carvedilol) used here. It was not possible to incorporate higher levels of carvedilol into these Soluplus nanofibers by electrospinning.

3.3.3. Fourier transform infrared spectroscopy

Fourier transform infrared spectroscopy was performed to study the interactions between carvedilol and Soluplus in the carvedilol-loaded Soluplus nanofibers obtained. Formulations with the lowest (N1, 5%) and highest (N6, 50%) percent of carvedilol are presented on the figure, as well as the Soluplus and carvedilol (Fig. 8).

The FTIR spectrum of pure carvedilol showed an intense, well-defined, characteristic infrared absorption band at 3344.5 cm^{-1}, which corresponded to the N–H stretching vibration of the secondary amine. Three intense absorption bands were at 2993.87 cm^{-1} and 2924.5 cm^{-1}, and at 1099 cm^{-1}, which corresponded to C–H aliphatic stretching and to C–O stretching, respectively. In addition, there were other sharp bands at 1500 cm^{-1} to 1400 cm^{-1}, as C–C aromatic stretching, and 1253 cm^{-1}, as C–N stretching.

Soluplus showed peaks at 3448.72 cm^{-1}, as O–H stretching, 2927.98 cm^{-1}, as aromatic C–H stretching, 1735.93 cm^{-1} and 1635.23 cm^{-1}, as C–O stretching, and 1477.21 cm^{-1}, as C–O–C stretching.

The FTIR spectra of these carvedilol-loaded Soluplus nanofibers in the form of this solid dispersion did not show the characteristic peak for carvedilol at 3344.5 cm^{-1} that corresponds to the N–H stretching. This can be attributed to a possible interaction between the –NH group of carvedilol and the –CO group of Soluplus, which would lead to the formation of an amide group in the nanofibers, as reported previously (Shamma and Basha, 2013).

3.3.4. In-vitro *dissolution study*

Carvedilol is a poorly soluble active substance, and this formulation as nanofibers with Soluplus showed improved dissolution properties according to *in-vitro* tests (Fig. 9). It can be noted that for all six of these formulations, >85% of the carvedilol was released in the first 15

min, and >95% at the end of the 1-h dissolution testing. The dissolution studies of pure carvedilol showed <40% released in 1 h, which demonstrates that these carvedilol-loaded Soluplus nanofibers have improved carvedilol dissolution. Thus these dissolution studies showed high percentages of dissolved carvedilol, which was most likely as a result of the solid dispersions formed by the electrospinning.

High percentages of incorporated carvedilol have been reported in the literature, at up to 60%, based on the dry weight of the polymer, polycaprolactone, but with higher percentages of chloroform used as solvent (Potrč et al., 2015). According to the data shown in Figure 9, the largest differences in the dissolution profiles between these formulations was in the first 15 min of dissolution. After these 15 min, the further release of carvedilol was similar across all of the formulations here, which ranged from 5% to 50% carvedilol. These data thus demonstrate that when the solid dispersion samples (i.e., the carvedilol-loaded Soluplus nanofibers) contain up to 50% carvedilol, immediate release of carvedilol can occur, and the carvedilol dissolution properties are improved in comparison to pure carvedilol.

4. Conclusions

The present study investigated different steps in the preformulation phase for obtaining different forms of carvedilol-loaded Soluplus nanofibers using electrospinning. Estimation of the miscibility of drug and polymer shown that a certain level of miscibility of carvedilol and Soluplus was expected and achieved. This justifies the formulation of such solid dispersions that contain these two components, in terms of the poor aqueous solubility of carvedilol. The Soluplus solubility map was constructed on the triangular graph, and the solvents were also assessed in terms of their carvedilol solubility and whether their dielectric constant was favorable for the electrospinning. This has not previously been reported in the literature and it allowed the formation of a specific database for the active pharmaceutical ingredient (i.e., carvedilol) and the chosen specific polymer (i.e., Soluplus) for the electrospinning. Moreover,

the data obtained from the Soluplus solubility map represents a step forward for estimation of the production of nanofibers by electrospinning using other active pharmaceutical ingredients that might or might not have similar properties to carvedilol. The approach presented here provides a less time-consuming process for the selection of a suitable solvent system.

It was found that the optimal solvent system for electrospinning of carvedilol and Soluplus is acetone: chloroform, 9:1 (w/w). Examination of the morphology of the nanofibers obtained showed no defects, and the electrospinning was stable throughout this process. Characterization of nanofibers revealed that the carvedilol in the carvedilol-loaded Soluplus nanofibers was in its amorphous state, with molecular dispersion throughout the Soluplus polymer through the formation of a miscible system. This was practical confirmation of the results of miscibility analysis of carvedilol and Soluplus. Also, carvedilol dissolution properties were improved, shown through dissolution tests of these carvedilol-loaded Soluplus nanofibers.

Therefore, the data from the present study support this drug formulation design, which includes improved prediction of the *in-vivo* carvedilol dissolution, to help to assure product efficacy and safety for patients.

Acknowledgments

This study was supported by Project TR34007, funded by the Ministry of Education, Science and Technological Development, Republic of Serbia.

References

Augustine, R., Kalarikkal, N., Thomas, S., 2016. Clogging-free electrospinning of polycaprolactone using acetic acid/ acetone mixture. Polym. Plast. Technol. Eng. 55, 518–529.

Balogh, A., Cselkó, R., Démuth, B., Verreck, G., Mensch, J., Marosi, G., Nagy, Z.K., 2015. Alternating current electrospinning for preparation of fibrous drug delivery systems. Int. J. Pharm. 495, 75–80.

Barton, A.F.M., 1983. Handbook of Solubility Parameters and Other Cohesion Parameters. CRC Press Inc. Boca Raton, Florida, USA.

Burke, J., 1984. Solubility parameters: theory and application, in: Jensen C (Ed). AIC Book and Paper Group Annual, 3, 13–58.

Chakraborty, S., Liao, I.C., Adler, A., Leong, K.W., 2009. Electrohydrodynamics: a facile technique to fabricate drug delivery systems. Adv. Drug. Deliv. Rev. 61, 1043–1054.

Djuris, J., Nikolakakis, I., Ibric, S., Djuric, Z., Kachrimanis, K., 2013. Preparation of carbamazepine–Soluplus® solid dispersions by hot-melt extrusion, and prediction of drug–polymer miscibility by thermodynamic model fitting. Eur. J. Pharm. Biopharm. 84, 228–237.

Greenhalgh, D.J., Williams, A.C., Timmins, P., York, P., 1999. Solubility parameters as predictors of miscibility in solid dispersions. J. Pharm. Sci. 88, 1182–1190.

Hansen, C.M., 2007. Hansen Solubility Parameters: a Users Handbook. 2nd ed. Boca Raton, CRC Press Inc. Florida.

Hardung, H., Djuric, D., Ali, S., 2010. Combining HME and solubilization: Soluplus® – the solid solution. Drug Deliv. Technol. 10, 20–27.

Jaeger, R., Bergshoef, M.M., Batlle, C.M.I., Schönherr, H., Julius Vancso, G., 1998. Electrospinning of ultrathin polymer fibers. Macromol. Symp. 127, 141–150.

Luo, C.J., Nangrejo, M., Edirisinghe, M., 2010. A novel method of selecting solvents for polymer electrospinning. Polymer 51, 1654–1662.

Luo, C.J., Stride, E., Edirisinghe, M., 2012. Mapping the influence of solubility and dielectric constant on electrospinning polycaprolactone solutions. Macromolecules 45, 4669–4680.

Mahalingam, S., Raimi-Abraham, B.T., Craig, D.Q., Edirisinghe, M., 2015. Solubility–spinnability map and model for the preparation of fibres of polyethylene (terephthalate) using gyration and pressure. Chem. Eng. J. 280, 344–353.

Marsac, P.J., Shamblin, S.L., Taylor, L.S., 2006. Theoretical and practical approaches for prediction of drug–polymer miscibility and solubility. Pharm. Res. 23, 2417–2426.

Marsac, P.J., Li, T., Taylor, L.S., 2009. Estimation of drug–polymer miscibility and solubility in amorphous solid dispersions using experimentally determined interaction parameters. Pharm. Res. 26, 139–151.

Meng, F., Dave, V., Chauhan, H., 2015. Qualitative and quantitative methods to determine miscibility in amorphous drug–polymer systems. Eur. J. Pharm. Sci. 77, 106–111.

Nagy, Z.K., Balogh, A., Vajna, B., Farkas, A., Patyi, G., Kramarics, Á., Marosi, G., 2012. Comparison of electrospun and extruded Soluplus®-based solid dosage forms of improved dissolution. J. Pharm. Sci. 101, 322–332.

Nagy, Z.K., Balogh, A., Démuth, B., Pataki, H., Vigh, T., Szabó, B., Verreck, G., 2015. High-speed electrospinning for scaled-up production of amorphous solid dispersion of itraconazole. Int. J. Pharm. 480, 137–142.

Paaver, U., Tamm, I., Laidmäe, I., Lust, A., Kirsimäe, K., Veski, P., Kogermann, K., Heinämäki, J., 2014. Soluplus graft copolymer: potential novel carrier polymer in electrospinning of nanofibrous drug delivery systems for wound therapy. BioMed. Res. Int. 2014, 789765.

Pelipenko, J., Kocbek, P., Kristl, J., 2015. Critical attributes of nanofibers: preparation, drug loading, and tissue regeneration. Int. J. Pharm. 484, 57–74.

Pham, Q.P., Sharma, U., Mikos, A.G., 2006. Electrospinning of polymeric nanofibers for tissue engineering applications: a review. Tissue Eng. 12, 1197–1211.

Potrč, T., Baumgartner, S., Roškar, R., Planinšek, O., Lavrič, Z., Kristl, J., Kocbek, P., 2015. Electrospun polycaprolactone nanofibers as a potential oromucosal delivery system for poorly water-soluble drugs. Eur. J. Pharm. Sci. 75, 101–113.

Ramakrishna S., Fujihara K., Teo W.E., Lim T.C. and Ma Z., 2005. An Introduction to Electrospinning and Nanofibers. World Scientific. Singapore.

Reneker, D.H., Chun, I., 1996. Nanometre diameter fibres of polymer, produced by electrospinning. Nanotechnology. 7, 216.

Reneker, D.H., Yarin, A.L., 2008. Electrospinning jets and polymer nanofibers. Polymer. 49, 2387–2425.

Shamma, R.N., Basha, M., 2013. Soluplus®: A novel polymeric solubilizer for optimization of carvedilol solid dispersions: formulation design and effect of method of preparation. Powder Technol. 237, 406–414.

Smallwood, I.M., 1996. Handbook of Organic Solvent Properties. Halsted Press, New York, USA.

Son, W.K., Youk, J.H., Lee, T.S., Park, W.H., 2004. The effects of solution properties and polyelectrolyte on electrospinning of ultrafine poly (ethylene oxide) fibers. Polymer 45, 2959–2966.

Stefanis, E., Panayiotou, C., 2012. A new expanded solubility parameter approach. Int. J. Pharm. 426, 29–43.

Teas, J.P., 1968. Graphic analysis of resin solubilities. J. Paint Technol. 40, 19–25.

Vasconcelos, T., Sarmento, B., Costa, P., 2007. Solid dispersions as strategy to improve oral bioavailability of poor water soluble drugs. Drug Discov. Today 12, 1068–1075.

Vo, C.L.N., Park, C., Lee, B.J., 2013. Current trends and future perspectives of solid dispersions containing poorly water-soluble drugs. Eur. J. Pharm. Biopharm. 85, 799–813.

Wannatong, L., Sirivat, A., Supaphol, P., 2004. Effects of solvents on electrospun polymeric fibers: preliminary study on polystyrene. Polym. Int. 53, 1851–1859.

Figure Caption

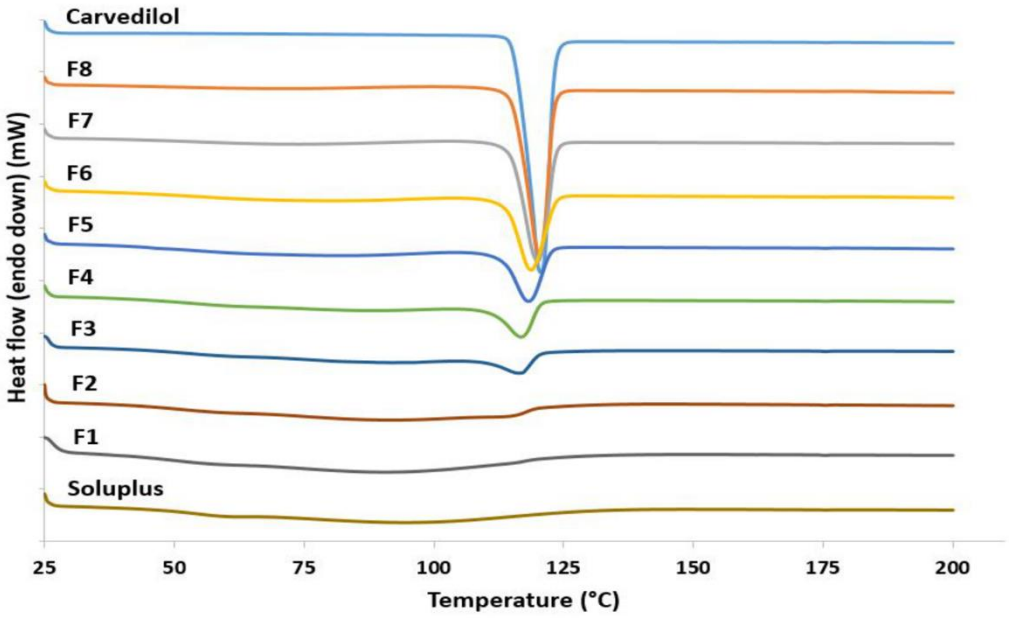

Figr-1

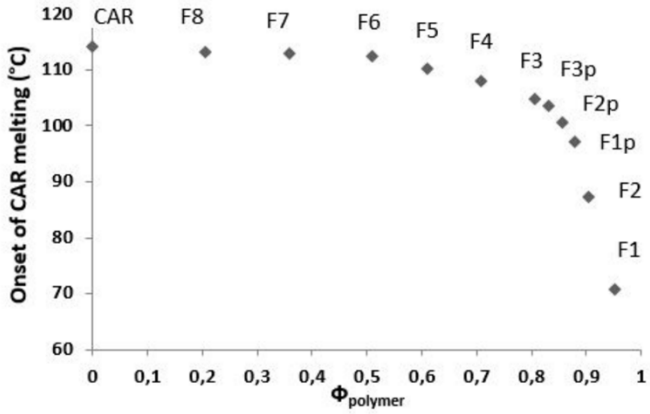

Figr-2

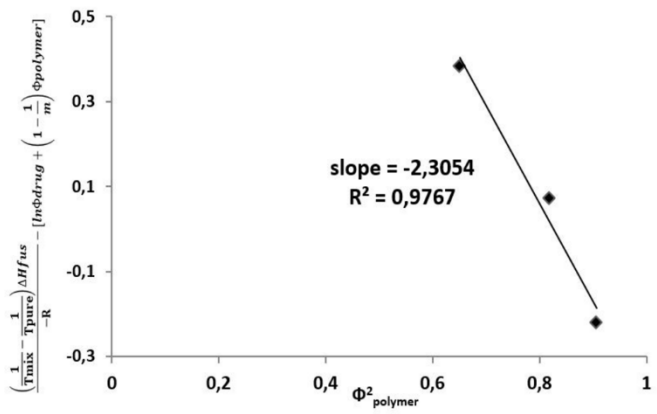

Figr-3

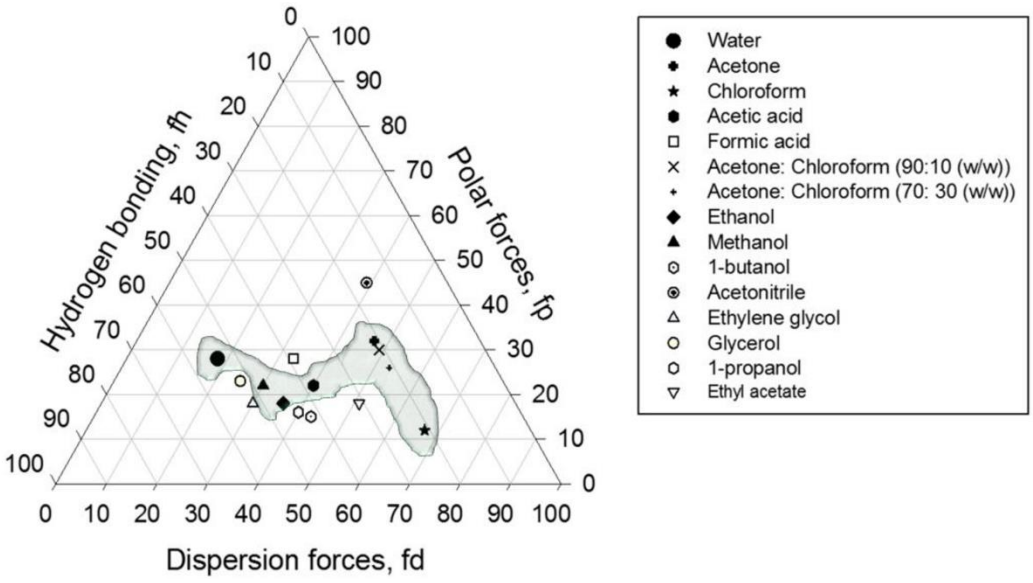

Figr-4

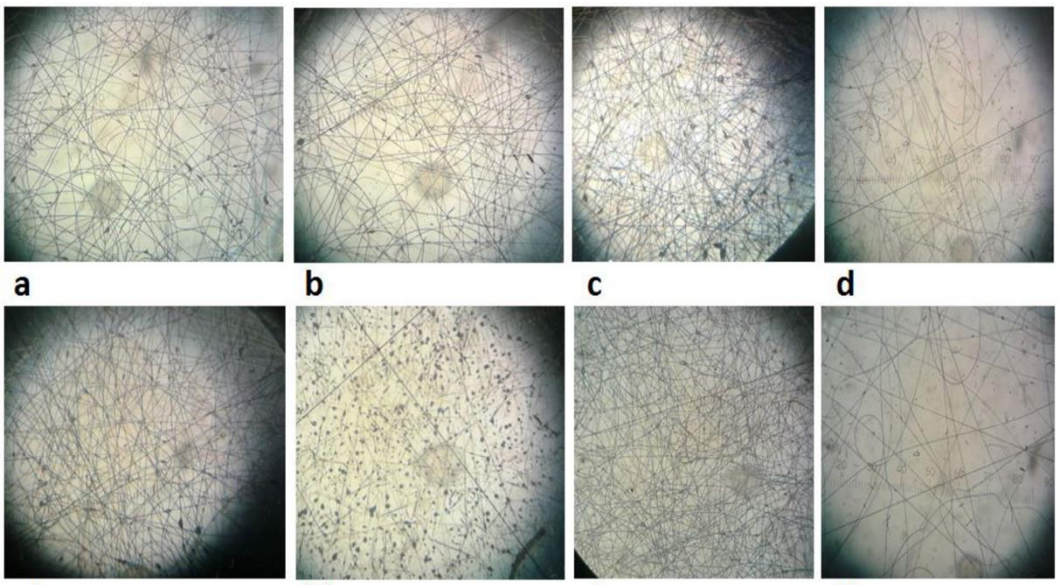

Figr-5

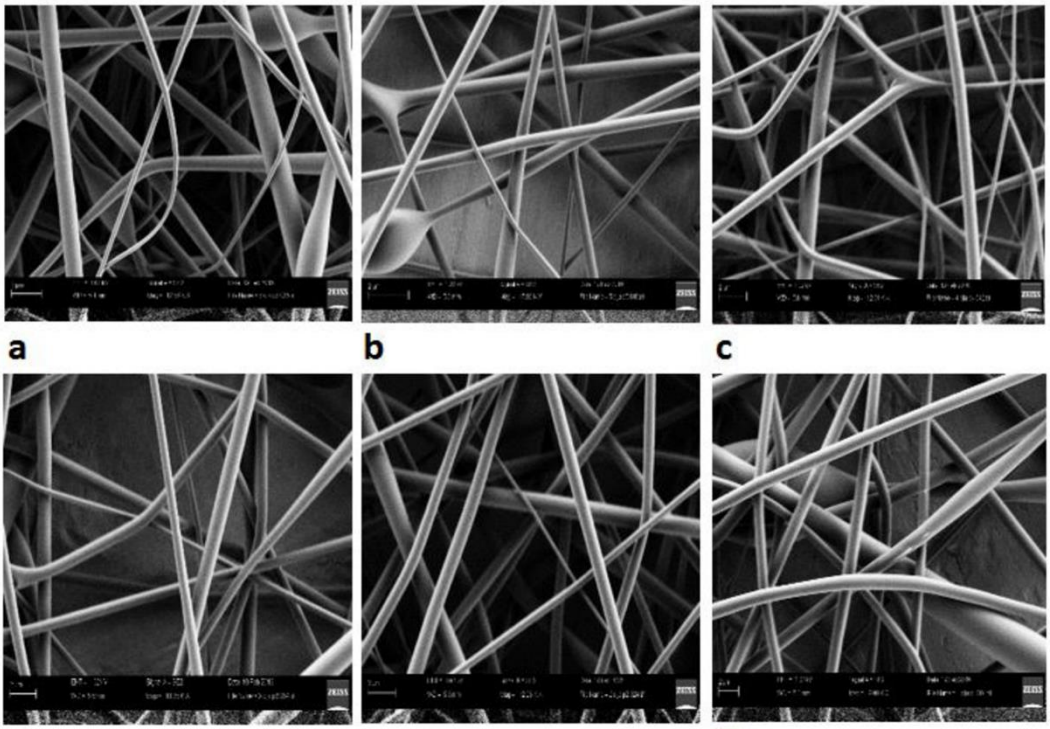

Figr-6

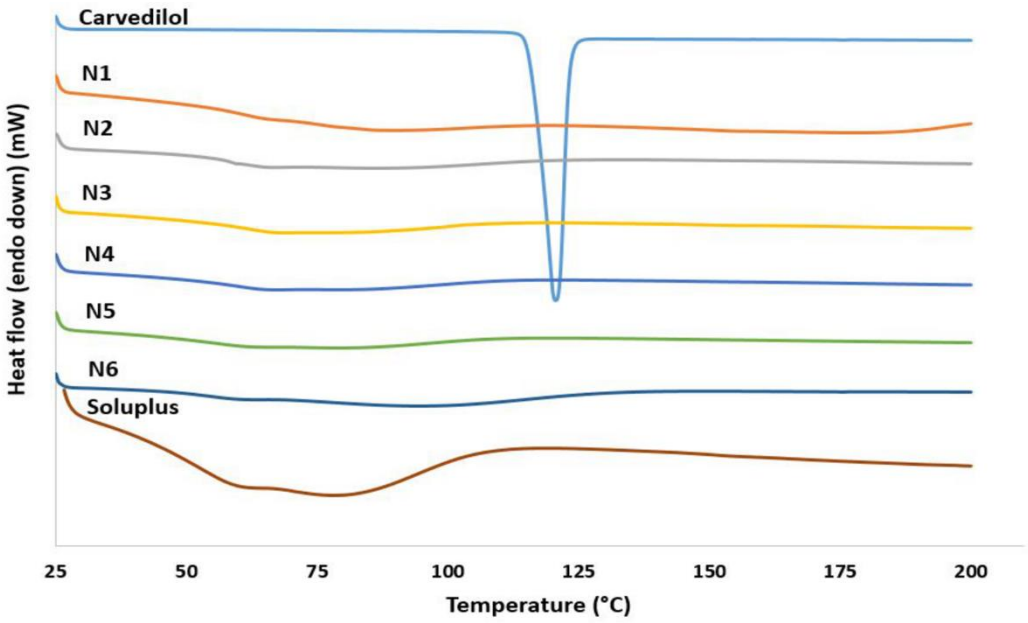

Figr-7

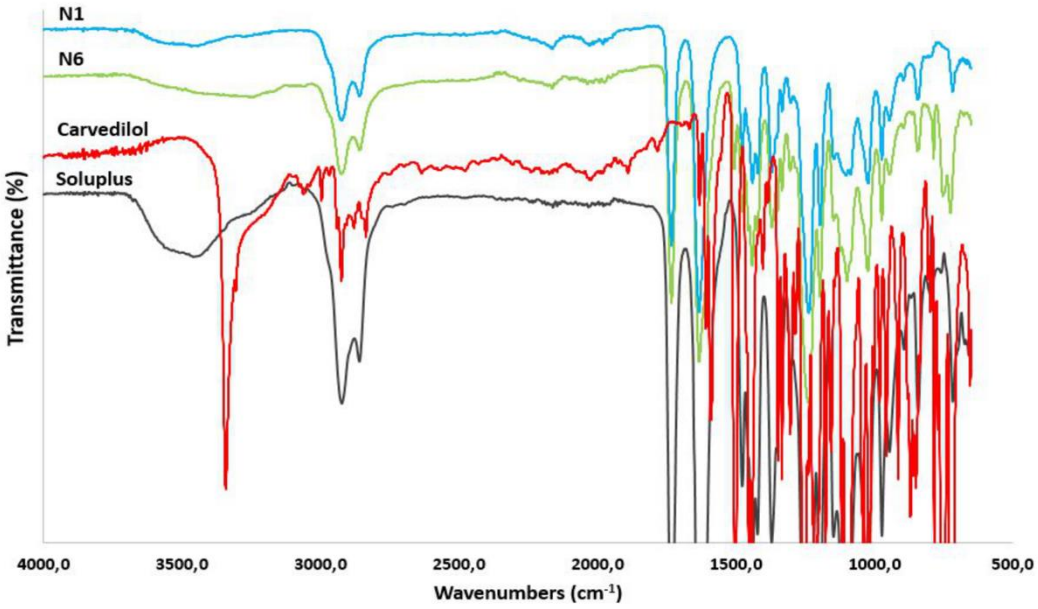

Figr-8

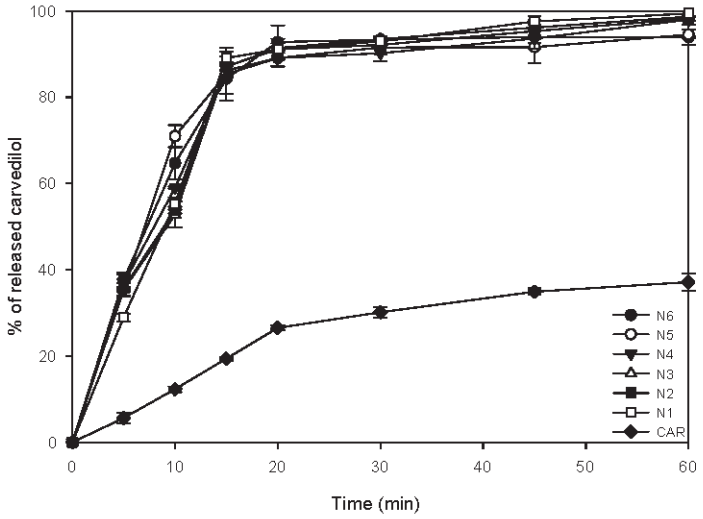

Figr-9

Table 1. Calculation of the fractional parameters for a 9:1 solvent mixture of acetone and chloroform (Barton, 1983).

Solvent	**Fractional parameter[a] calculation**		
	f_d	**f_p**	**f_h**
Chloroform	67 × 1/10 = 6.7	12 × 1/10 = 1.2	21 × 1/10 = 2.1
Acetone	47 × 9/10 = 42.3	32 × 9/10 = 28.8	21 × 9/10 = 18.9
Acetone: chloroform, 9:1	42.3 + 6.7 = **49**	28.8 + 1.2 = **30**	18.9 + 2.1 = **21**

Table 2. Electrospinning parameters used for the nanofiber production

Carvedilol (%)	**Flow rate (ml/h)**	**Applied voltage (kV)**
5	4	14
10	2	12
20	2	14
30	1	11
40	2	13

50	1	11

Table 3. The solubility parameters for carvedilol and Soluplus.

Compound	**Solubility parameter ($MPa^{1/2}$)**			
	δ_d	**δ_p**	**δ_h**	**δ_t**
Carvedilol	19.5	7.6	7.6	22.3
Soluplus	17.4	0.3	8.6	19.4

Table 4. The chosen solvents and their properties.

Solvent system	**Dielectric constant (ε_r)**	**Carvedilol solubility[a]**	**Electrospinning suitability**
Acetone	20.6	S	Formed beads
Chloroform	4.9	S	Unsuitable
Acetone: chloroform, 9:1 (w/w)	19.03	S	Formed nanofibers
Acetone: chloroform, 7:3 (w/w)	15.89	S	Formed beads
Ethanol	24.5	S	Formed beads
Methanol	32.6	S	Formed particles
Acetic acid	6.2	I	Unsuitable
Water	79	I	Unsuitable

Figr-10**Figure 1.** Thermograms of carvedilol, Soluplus® and physical mixtures. These were prepared as 10 g of each pure mixture and by manual addition of carvedilol and Soluplus to different carvedilol percentages (g, percentage carvedilol): F1, (5%); F2, (10%); F3, (20%); F4, (30%); F5, (40%); F6, (50%); F7, (65%); and F8, (80%).

Figure 2. Depression of the onset of the carvedilol melting temperature with increase in Soluplus volume fraction. As for Figure 1: F1, (5%); F2, (10%); F3, (20%); F4, (30%); F5, (40%); F6, (50%); F7, (65%); and F8, (80%). Additional data points: F1p, (12.5%); F2p, (15%); F3p, (17.5%).

Figure 3. Plot used to calculate the carvedilol–Soluplus miscibility interaction parameter χ.

Figure 4. Triangular graph for determination of the Soluplus solubility map.

Figure 5. Representative carvedilol-loaded Soluplus nanofibers observed under optical microscopy during the solvent selection: (a, a') ethanol; (b, b') methanol; (c, c') acetone, (d, d') acetone: chloroform (90: 10, w/w).

Figure 6. Representative carvedilol-loaded Soluplus nanofibers observed in scanning electron microscopy micrographs, using different percentages of carvedilol (a–f): a) N1, (5%); b) N2, (10%); c) N3, (20%); d) N4, (30%); e) N5, (40%); f) N6, (50%).

Figure 7. Differential scanning calorimetry thermograms for pure carvedilol and Soluplus, and for the nanofibers from the different carvedilol percentages (g, percentage carvedilol): N1, (5%); N2, (10%); N3, (20%); N4, (30%); N5, (40%); N6, (50%).

Figure 8. Representative spectra from Fourier transform infrared spectroscopy of carvedilol, Soluplus, and the nanofiber with the lowest and highest percent of carvedilol (g, percentage carvedilol): N1, (5%); N6, (50%).

Figure 9. *In-vitro* dissolution profiles of carvedilol from the nanofibers from the different carvedilol percentages (g, percentage carvedilol): N1, (5%); N2, (10%); N3, (20%); N4, (30%); N5, (40%); N6, (50%), and for pure carvediol.